Effect of SrO on the thermal, optical and structural properties of sodium borosilicate glasses

Dissertation submitted in partial fulfillment

of the requirement for the degree of

Master of Science

in

Physics

Submitted By:

Simranjeet Kaur

Roll Number- 301904016

Under the supervision of:

Dr. Kulvir Singh

Professor and Associate Dean

(Research and Sponsored Projects)

School of Physics and Materials Science

Thapar Institute of Engineering and Technology, Patiala

Punjab-147004, India

July-2021

Dedication

This dissertation with all my heart is dedicated firstly to almighty **GOD** and then, to my beloved parents and siblings.

Simranjeet Kaur

Certificate

I Simranjeet Kaur, roll number 301904016 hereby declare that this dissertation entitled "Effect of SrO on the thermal, optical and structural properties of sodium borosilicate glasses" presents my original work carried out in partial fulfillment of the requirements for the award of the degree of Master of Science in Physics submitted to the School of Physics and Material Science, Thapar Institute of Engineering and Technology, Patiala, Punjab. This is an original report and has not been submitted for any degree to this or any other institute. Any contribution by others to this research work are acknowledged in this dissertation and work of other authors are cited in this dissertation under the sections "References" or "Bibliography".

July, 2021

Thapar Institute of Engineering and Technology,

Patiala, Punjab

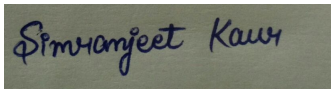

Simranjeet Kaur

This is to certify that the above statement made by the candidate is correct and true to the best of my knowledge.

Prof. Kulvir Singh

School of Physics and Materials Science

Thapar Institute of Engineering and Technology, Patiala-147004

Acknowledgement

I would like to begin this by expressing my deep and sincere gratitude to my research supervisor **Dr. Kulvir Singh**, Professor and Associate Dean (Research and Sponsored Projects), School of Physics and Material Science, Thapar Institute of Engineering and Technology, Patiala, Punjab for his invaluable advice, support, stimulating discussion and continuous motivation. He regularly monitored my work despite of his busy schedule. His attention towards my work, ideas, blessings and faith in me made me more confident to successfully complete my work during this pandemic period. It gives me immense delight to express my special thanks to **Ms. Manmeet Kaur** (Research scholar) who supported and guided me throughout this journey with the best of her knowledge and experience which helped me to complete my work. I am also thankful to **Ms. Shivani Punj** who also helped me with her knowledge and experience in the present research work. I would like to thank **Ms. Trisha Walia** and **Ms. Vimmi Dua** for their kind help.

I am also thankful to **Mr. Savidh Khan, Ms. Paramvir Kaur, Ms. Taranveer Kaur** for guiding me at various stages throughout the journey.

Simranjeet Kaur

Abstract

In the present work, borosilicate glasses ($29SiO_2 - 20B_2O_3 - 24.5Na_2O - (24.5 - x)CaO - xSrO - 2ZrO_2$ where, x=0, 5, 10, 15 wt%) synthesized by melt-quench technique are characterized by differential thermal analyzer (DTA), Fourier transform infrared spectroscopy (FTIR) and diffused reflectance spectroscopy (DRS) to study their structural, thermal, and optical properties. DTA is used to study the effect of SrO/CaO ratio on the glass transition and crystallization temperatures. The changes in the local structure (short range order) of glass is observed by FTIR spectroscopy. The values of optical band gap calculated by DRS results lie in the wide band gap semiconductor range. These properties help to understand the effect of SrO on the structural, thermal, and optical properties which can influence the bioactive behavior of the glasses.

KEYWORDS- Sodium borosilicate glass, Glass transition, UV-Vis spectroscopy

List of Acronyms

NBOs - Non Bridging Oxygens

BOs - Bridging Oxygens

DTA - Differential Thermal Analysis

FTIR - Fourier Transform Infrared Spectroscopy

DRS - Diffused Reflectance Spectroscopy

T_g - Glass Transition Temperature

T_c - Onset Crystallization Temperature

T_p - Peak Crystallization Temperature

E_g - Optical Band Gap

E_u - Urbach Energy

n - Refractive Index

n_1 - Refractive index calculated from direct E_g value

n_2 - Refractive index calculated from indirect E_g value

SOFCs - Solid Oxide Fuel Cells

HCA - Hydroxy Carbonate Apatite

HAp - Hydroxy Apatite

BG - Bioactive Glass

SBF - Simulated Body Fluid

SEM - Scanning Electron Microscopy

XRD - X ray Diffraction

EDS - Energy Dispersive x ray Spectroscopy

μ V - Micro Volt

F(R) - Kubelka Munk Function

α - Absorption Coefficient

β - Constant

s - Scattering Coefficient

R - Reflectance

h ν - Energy of photon

Contents

List of Figures

List of Tables

Chapter 1

Introduction

Glasses are super-cooled liquids/amorphous solids, lacking any long range order, and are brittle, transparent or translucent in nature. They possess a glass transformation behaviour which is time dependent and occurs over a temperature range which is called as glass transformation region [1, 2]. The value of viscosity at glass transformation temperature is $10^{11.3}$ Pa s [3]. The variation in range of glass transformation depends on different factors like composition, melting temperature, viscosity, and cooling rate of the substance [4]. Glasses find use in solid oxide fuel cells [5], solid-state lighting [6], biomaterials [7], photocatalysis [8], etc. Glass has three main components which are named as glass formers, glass modifiers and intermediates [3]. They are differentiated according to their electronegativities and bond energies or bond strength of constituents in the glass structure. Glass formers build the glass network and they possess the highest electronegativity and bond strength out of these three components and are able to form 3D structures [3, 4]. SiO_2, B_2O_3, P_2O_5 are the examples of common formers [4, 5, 9]. Cations having lower electronegativity than the formers are able to form bonds with the oxygen which will modify the glass structure are known as modifiers. They break down the network of the glass with the creation of terminal oxygens which are known as non-bridging oxygens (NBOs) [3, 4]. Some common examples of modifiers are $Na_2O, Li_2O, CaO, BaO, SrO, MgO$ [4, 9]. Cations forming bonds with oxygen having electronegativity more than that of modifiers and less than formers are called as intermediates [3]. Intermediates can play the role of either former or modifier in the glass network depending on the glass composition and their amounts [4]. Al_2O_3, ZrO_2 are the examples of intermediates [4, 9].

The most common technique used to synthesize a glass is melt-quench technique [3]. In the melt-quench technique, glass is prepared by taking essential amounts of constituent oxides or carbonates having higher purity. Then, by using ball mill in an acetone medium, these constituents are mixed [1]. The powder obtained by ball milling is then heated in a high resistance furnace at high temperature depends on the composition. The melt is then poured into a mold to obtain desired shape of the glass [1, 10]. Then, in air, quenching of melt is done by using copper plates. The quenched glass is annealed at a relevant temperature in order to remove internal stress from glass. Different

properties of glasses like glass stability, density, solubility are affected by the structure of the glass. Addition of some oxides to the glass composition, i.e. doping helps to change the properties of the glass according to a particular application [4].

Glass transition temperature (T_g), peak crystallization temperature (T_p) and onset crystallization temperature (T_c) are determined by using Differential Thermal Analysis (DTA) technique [7, 11]. The temperature at which glass transition occurs is a particular temperature, at which there is a phase change from solid to viscous liquid occurs [4]. T_g depends on heating rate and composition of the glass [3, 7, 11]. Optical band gap (E_g), refractive index (n) and Urbach energy (E_g) are determined by using diffuse reflectance spectra (DRS) [9, 12]. E_g depends on the glass composition and NBOs present in the structure of the glass [13, 14, 15, 16, 17]. Urbach energy (E_u) depends upon glass composition, defects and disorder present in the glass [13, 14, 15, 17]. Refractive index (n) depends on density, composition, ionic and molar refractivity, coordination number, field strength, NBOs and the presence of polarizability of anions in the glass [5, 14, 15, 18]. It is a structure dependent property [5].

SiO_2 is most widely used former. In silicate glasses, Si is in tetrahedral coordination with the oxygen which is a basic building block [4, 19]. Due to linkage at all four corners, these tetrahedra form a continuous 3D network [20]. Si-centred tetrahedrally is assigned as Q^n, where, Q denotes to atom of silicon and n denotes to number of bridging oxygens (BOs). Q^0 structural species are SiO_4^{4-} monomers, Q^1 structural species are $Si_2O_7^{6-}$ dimmers, Q^2 structural species are SiO_3^{2-}, Q^3 structural species are $Si_2O_5^{2-}$ sheets and Q^4 structural species are SiO_2 tetrahedral configuration [19]. The addition of network modifiers in the glass composition causes a disturbance in the glass network. This leads to cleavage of some Si-O-Si bonds and hence, NBOs are formed [4]. The higher number of NBOs present in the glass structure leads to a weaker structure. This is because of decrease in BOs and network connectivity [4, 12]. The addition of network modifiers also lead to decrease in T_g [3]. Silicate glasses can be used in bone tissue engineering [21]. 45S5 glass composition was the first bioglass (BG) developed by Hench which is used for different applications like middle ear prosthesis, dentistry, and orthopedic applications [1, 20, 22, 23].

B_2O_3 is another commonly used network former. In borate glasses, boron occurs in both triangular and tetrahedral coordination. With the addition of network modifiers, boron changes its coordination from triangular to tetrahedral without forming NBOs and hence, causes an increase in network connectivity and also in T_g. But with the higher addition of network modifiers, properties show reverse trend. This phenomenon is termed as boron anomaly. Borate glasses are applicable in the

field of optical communications, optical filters, lasers, photonic devices and biomedical applications etc. [24, 25].

When a significant amount of B_2O_3 is present in the glass along with SiO_2, then the sample is called as borosilicate glass. The structure of borosilicate glasses begins with the consideration of compositional regions of heterogeneous (phase separated) and homogeneous glasses. The heterogeneous borosilicate glass has two phases one phase is silica rich and other is boric acid phase. In borosilicate glasses, BO_3 structural units are formed during annealing which then form boroxyl rings by connecting with each other. This can cause a decrease in NBOs and an increase in E_g [15]. Borosilicate glasses are used for applications due to their better chemical durability, electrical resistivity and thermal shock resistance [3]. Borosilicate glasses are suitable to use as sealants in solid oxide fuel cells (SOFCs) if their optical band gap is less than 2.5 eV and in biomedical applications [5, 26].

Glasses are important for applications as biomaterial. Biomaterials are used in orthopedic applications, skin grafting, dentistry, knee replacement etc [7, 27]. Any material other than drugs which is capable of improving the condition of the human body by restoring or partially or completely replacing part of living tissue or system in an intimate contact with the living tissue used for any period of time is defined as a biomaterial [28, 29]. The response of the biomaterial in-vitro and in-vivo testing should be known before using it as an implant since the implant should remain in contact with the tissue without releasing any substances which can cause harm to the tissues. In other words, biomaterial should be biocompatible and non-toxic [27, 30]. Biocompatibility can also be defined as the acceptance of an artificial implant by the surrounding tissues in the human body [28]. Biomaterials are of three types- (1) bioinert, (2) biodegradable and (3) bioactive. The biomaterials which do not show any significant interaction with the surrounding tissues are named as bioinert biomaterials. These materials have applications in orthodontics [7]. Stainless steel, partially stabilized zirconia and polyethene, alumina, titanium, bioinert alumina as dental implant are examples of bioinert materials [31]. The biomaterial which dissolves or degrades after implantation inside the human body are named as biodegradable biomaterials [7]. For example, polymeric materials [31]. The biodegradable materials are used as fillers in cracks and are widely used to repair bone defects [7]. Bioactive materials are those materials which obtain a particular biological response at the interface of the material that leads to form a significant bond between the tissues and the material [32]. For example, bioactive glasses, hydroxyapatite (HAp) [22].

Hench et al. [22] developed the first bioactive glass in 1969 with the glass composition $45SiO_2 - 24.5Na_2O - 24.5CaO - 6P_2O_5$ (wt%) [22]. Here, Ca/P ratio is same as of bone [33]. During physio-

chemical process, BG undergoes leaching, dissolution and precipitation releasing some ions and forming hydroxy carbonate apatite (HCA) layer. The formation of HCA confirms that the bonding with the tissue takes place [22, 34]. The major components of human bone are HAp ($Ca_{10}(PO_4)_6(OH)_{10}$) which is a hard though brittle material and other is collagen (a protein) which is a flexible and soft material [35, 36]. That's why formation of HAp is important. The 45S5 glass suffers from some drawbacks like low mechanical strength, slow rate of degradation and limited ability of densification accompanied with crystallization during sintering [7, 20, 37, 38, 39, 40]. Still there is a lot of interest in improving properties of this glass. Due to applications of BG in various fields, lots of research is being carried out to improve the properties of the bioglass.

Chapter 2

Literature Survey

The literature has been reviewed correlated to the present work and discussed in this chapter. After the publication of first research paper in 1969, the bioglass has got attention. The work done by other researchers and applications and pros and cons of their work has also been given which led us to decide the present composition .

Hench et al. [22] synthesized the first bioglass which is known as bioactive glass (BG) of the glass composition $45SiO_2 - 24.5Na_2O - 24.5CaO - 6P_2O_5$ (wt%). This composition is known as 45S5 where, S denotes to the network former silicon dioxide (SiO_2) and 5 represents the Ca/P ratio [22]. 45S5 BG is highly bioactive [20, 23], due to which a well mineralized HAp layer is formed when in contact with bodily fluid [20]. In 1984, 45S5 glass was clinically used for middle ear prosthesis [20, 41]. It was found that bone can chemically bond to certain glass compositions such as 45S5 glass synthesized by Hench [1, 22]. But 45S5 glass has slow degradation rate, i.e. BG degrades slowly than the rate of growth of the tissue after its implantation inside the human body and has poor mechanical strength. Due to lack of mechanical strength, 45S5 glass is not applicable for load bearing orthopedic applications [7, 20]. Another challenge is the limited densification ability of 45S5 glass associated with crystallization during sintering. This makes it difficult to shape the 45S5 glass into complicate structure at high temperatures [40]. That is why, it becomes important to analyze the crystallization mechanism of 45S5 glass to enhance its sinterability while keeping its bioactivity. Due to these limitations, it becomes important to modify the BG composition. Ohura et al. [42] developed phosphate-free silicate glass with the composition $48.3CaO - 51.7SiO_2$ wt% and phosphate-containing silicate glasses with the composition $43.1CaO - 50.8SiO_2 - 6.1CaF_2$ wt% and $43.1CaO - 50.2SiO_2 - 2.9P_2O_5$ wt%. It was found that both phosphate-free and phosphate-containing glasses have same ability of bone bonding and also no difference of bone bonding strength occurred between phosphate-free and phosphate-containing glasses [42]. Fredholm et al. [43] synthesized silicate glasses with the composition $49.46SiO_2 - 1.07P_2O_5 - (23.0 - X)CaO - XSrO - 26.38Na_2O$, X=0.0, 0.58, 2.31, 11.54, 23.08 mol%. It was concluded that the replacement of Ca by Sr causes a small change in the chemical structure of the glass and minor but significant expansion occurs in

the network of glass due to larger cation size of Sr^{2+} ion than that of Ca^{2+} ion. This results in the weakening of the glass structure and a decrease in glass transition temperature [43]. Huang et al. [44] synthesized glass with the composition $53SiO_2 - 6Na_2O - 12K_2O - 6MgO - 20CaO - 4P_2O_5$ wt% which is known as 13-93. This glass has requisite mechanical strength and compressive strength which is equivalent to human cortical bone. The glass is bioactive in nature and supports proliferation but suffers from reduced conversion rate to HAp. It has potential application in repair and regeneration of load bearing bones [44]. Jha et al. [45] synthesized $55SiO_2 - 10K_2O - (35 - x)CaO - xMgO$, x=5, 15, 25, 35 mol% glasses. It was found that chemical durability of the glasses increased but their bioactive properties retarded by replacing CaO with MgO [45]. Hesaraki et al. [46] developed glass with the composition of $64SiO_2 - 5P_2O_5 - (31 - x)CaO - xSrO$ where, x=0, 2, 5, 8, 10 mol%. The ionic radius of Ca ion (1.00 Å) is lower than that of Sr ion (1.13 Å). It was found that a degradable glass developed with the higher amount of Sr. The increase in T_g was found to be directly proportional to the amount of Sr present in the glass, but bioactivity of the glass retarded with the increasing Sr concentration [46].

In order to improve the degradation rate of the BG glass other network formers such as borate and phosphate have been used to replace partially or completely SiO_2 [20, 47]. Boron is a required trace element for bone [1, 48]. Boron is also found in hair and nails in the human body [48]. Due to lower cation size, small heat of fusion, high field strength and trivalent nature of boron in B_2O_3, it becomes an important glass forming oxides [4, 49]. Borate glasses have applications in clinical use as bone grafts [1]. The complete replacement of SiO_2 with B_2O_3 in BG results in higher degradation rate but lowers the durability and cytotoxicity because of the rapid release of boron [1, 47, 50]. Richard et al. [51] replaced SiO_2 with B_2O_3 in 45S5 glass composition [25, 51] and named it as 45S5B1 [52]. This borate glass displayed faster conversion to HAp layer and hence, promoted bone formation more rapidly than its silica counterparts [51, 52]. The network connectivity increased but the strength decreased for this borate glass [51]. Also, high amount of B_2O_3 in the glass can be toxic to the cells [50]. Abdel et al. [53] developed $(20 - x - y)Na_2O - 80B_2O_3 - xBaO - yMgO$, where either x or y=0, 5, 10 wt% glasses. It was observed that E_g and E_u increased as MgO or BaO increased in the glass. They have better optical properties and can be used in wave-guide applications [53]. Liang et al. [54] synthesized $Na_2O - CaO - B_2O_3$ glass. It was concluded that partially converted borate glass to HAp, i.e. formation of HAp with Ca/P ratio less than stoichiometric value 1.67 or completely converted borate glass to HAp promote attachment and differentiation of stem cells. Partially converted borate glass has greater metabolic activity than fully converted borate glass

and favourable characteristics for cell viability whereas fully converted borate glass has applications in bone tissue engineering [54]. Abdelghany et al. [25] synthesized glasses with the composition $70B_2O_3 - 15CaO - xNa_2O - yLi_2O - zK_2O$ where, (x, y, z)=(15, 0, 0), (0, 15, 0), (0, 0, 15) wt% and $75B_2O_3 - 45CaO$ wt%. It was concluded that B_2O_3 is a hygroscopic oxide and is highly soluble in water. The samples were corrosive in nature but the the addition of alkali oxide helped to improve this issue. The bioactivity of the glass depends upon factors like composition of the glass and type of modifiers in the glass [25]. Abdelghany et al. [55] synthesized glass with the composition $60B_2O_3 - (20 - x)CaO - (20 - y)Na_2O - (x + y)SrO$ where, x=y=0.0, 2.5, 5, 7.5, 10 wt%. It was observed that with the increment in the amount of SrO by replacing CaO and Na_2O, the glass had enhanced bioactivity. The apatite phase formed depending on the concentration of SrO present in the glass [55].

The partial replacement of SiO_2 with B_2O_3 is beneficial as borosilicate glasses have the ability to form HAp layer faster and have better mechanical properties [50, 56]. They have applications in tissue engineering due to their higher reactivity with biological fluids [50]. Brink et al. [56] developed a borosilicate glass $Na_2O - K_2O - MgO - CaO - B_2O_3 - P_2O_5 - SiO_2$ for biomedical applications. The composition was within the range 0 to 25 wt% of Na_2O, 0 to 15 wt% of K_2O, 0 to 5 wt% of MgO, 0 to 3 wt% of B_2O_3, 8 to 20 wt% of CaO, 39 to 70 wt% of SiO_2 and 0 to 6 wt% P_2O_5. This borosilicate glass was found to be bioactive, very reactive and maintained mechanical properties but had low chemical durability [56]. The T_g value showed an increase with the addition of small amount of boric acid to silica [3]. Huang et al. [52] synthesized glasses with the composition $24.4Na_2O - 26.9CaO - (46.1 - x)SiO_2 - xB_2O_3 - 2.6P_2O_5$, x=0.0, 15.4, 30.7, 46.1 mol%. The Ca/P ratio decreased which leads to faster conversion to HAp [52]. Brown et al. [57] developed glasses with the composition $24.4Na_2O - 26.9CaO - xB_2O_3 - (46.1 - x)SiO_2 - 2.6P_2O_5$ where, x=0.0, 15.4, 30.7, 46.1 mol%. It was observed that conversion rate increased with the increment in the amount of B_2O_3 in the glass. In borate glass, i.e. when x=0.0 mol%, little inhibition of cell proliferation occurred. But greater inhibition of cell proliferation in cultures happened when the amount of B_2O_3 increased in the glass [57]. Fu et al. [39] synthesized $(54.6 - x)SiO_2 - xB_2O_3 - 6Na_2O - 7.9K_2O - 7.7MgO - 22.1CaO - 1.7P_2O_5$, x=0, 18.2, 54.6 mol% glasses. In these glasses, with the increase in the amount of B_2O_3, rate of conversion to HAp became faster, bioactivity and degradation rate also increased but strength decreased. They can be used in repairing bone defects [39]. Prasad et al. [58] synthesized $(50 - x)SiO_2 - xB_2O_3 - 9.3Na_2O - 37CaO - 3.7P_2O_5$ where, x=0.0, 12.5, 25, 37.5 mol% glass. Addition of B_2O_3 in silicate glasses improved antibacterial properties and in-vitro

cell proliferation along with the better biomineralization ability [58]. It is expected that thermal stability ($T_c - T_g$) of glasses improves upon replacement of SiO_2 with B_2O_3. This is caused by the participation of modifiers between silicate and borate units. But in this particular composition the partial substitution of B_2O_3 with SiO_2 resulted in decrease in thermal stability. This is caused by the shifting of T_c towards low temperature due to phosphate crystallization.

In order to enhance the chemical, physical, and biomedical properties of the BG certain elements like strontium (Sr), silver (Ag), zinc (Zn), fluoride (F), aluminum (Al), zirconia (Zr) are introduced in the glass composition [4]. Mondal et al. [59] introduced zirconia in the glass composition: $xZrO_2 - 24.5CaO - 6P_2O_5 - 24.5Na_2O - (45 - x)SiO_2$ where, x=0, 3, 6, 10 wt%. The mechanical strength and fracture toughness increased and it was observed that up to 10wt.% ZrO_2 gave better mechanical strength and compatibility. They are used in load bearing applications [59]. Samudrala et al. [60] synthesized a borosilicate glass with the composition $31B_2O_3 - 20SiO_2 - 24.5Na_2O - (24.5 - x)CaO - xZrO_2$ where, x=0, 1, 3, 5 mol%. The hardness, chemical reactivity of the glass increased and had good bioactivity due to the addition of zirconia. Zr acts as modifier in the glass structure and leads to creation of NBOs but it improves strength of the glass due to formation of Zr-O-Si covalent bonds in the glass network of silica with the addition of ZrO_2 . The glass can be used as bioactive material in the medical field for potential applications [60].

Agathopoulos et al. [61] introduced strontium in the glass of composition $SiO_2 - B_2O_3 - CaO - MgO - P_2O_5 - Na_2O - CaF_2$. The components were in the range of 40.08-42.95 wt% of SiO_2, 4.52-5.33 wt% of B_2O_3, 29.10-32.80 wt% of CaO, 7.86-9.25 wt% of MgO, 2.77-6.32 wt% of P_2O_5, 4.03-4.74 wt% of Na_2O and 5.07-5.98 wt% of CaF_2. It was found that the samples are bioactive in nature [61]. Belluci et al. [62] synthesized glass with the composition $2.3Na_2O - 2.3K_2O - 45.6CaO - 2.6P_2O_5 - 47.2SiO_2$ (10 mol% of CaO replacing with MgO or SrO or MgO & SrO). These glasses had enhanced bioactivity with the replacement of Ca by Sr and possessed good mechanical properties. It was concluded that no structural changes occur with the replacement. They promote bone formation, reduce bone resorption and are applicable for dental implants and bone regeneration [62]. Kargozar et al. [50] added strontium in the glass composition $SiO_2 - P_2O_5 - CaO - Na_2O - SrO$. It was concluded that Sr enhances rate of apatite layer formation and Sr^{2+} ions have antibacterial properties [50]. Gautam et al. [63] synthesized glass with the composition $(60 - x)[SrTiO_3] - 39[2SiO_2B_2O_3] - (1 + x)TeO_2$, where, x = 0, 2, 4, 6 and 8 mol%. It was concluded that number of NBOs increased when fraction of BO_4 units decrease within the borate network. The formation of NBOs leads to decrease in E_g values [63]. Sr addition is beneficial to reduce bone resorption. They are applicable in dental applications

[62].

Mohini et al. [48] synthesized glass with the $(55-x)B_2O_3-5SiO_2-20CaO-20Na_2O-xSrO$ composition where, x=2, 4, 6, 8, 10 mol%. It was found that SrO acts as a modifier resulting in formation of NBOs and reduction in the value of E_g [48]. Kaur et al. [15] synthesized $(10+x)CaO-(10-x)MgO-10SrO-10B_2O_3-20Al_2O_3-40SiO_2$, x=0, 2.5, 5, 7.5 mol% glasses. It was found that the values of E_g and E_u increased as the amount of CaO/MgO in the glass increased. Khan et al. [9] prepared a glass with the composition $30SiO_2-30B_2O_3-10Y_2O_3-(30-x)CaO-xZrO_2$ where, x=2.5, 5, 7.5, 10 mol%. In this glass, E_g decreases as NBOs increases in the structure of the glass and higher the disorder in the glass, higher is the value of E_u. This borosilicate glass is useful in optical switches [9]. Walia et al. [5] synthesized borosilicate glass with the composition $(40-x)SrO-xBaO-45SiO_2-10B_2O_3-5ZrO_2$, x=0, 10, 20, 30, 40 mol%. It is expected that E_g decreases as the alkaline ion concentration increases in single alkaline borosilicate glasses. But a non-linear variation in the E_g value with the decreasing in SrO concentration was reported due to the existence of mixed alkali effect [5].

Fujikura et al. [64] synthesized $46.1SiO_2-2.5P_2O_5-(26.9-x)CaO-xSrO-24.4Na_2O$ where, x=0, 6.7, 13.5, 20.2, 26.9 mol% bioactive glasses. According to the DSC results with the increasing SrO concentration T_g value decreased. Since Sr^{2+} has ionic radius slightly larger than calcium, the Sr-containing glasses are more disturbed which leads to a decrease in T_g [64]. Tainio et al. [65] prepared bioactive borosilicate glass with the composition $47.2SiO_2-6.73B_2O_3-(21.77-x-y)CaO-22.65Na_2O-1.72P_2O_5-xMgO-ySrO$ where, (x, y)=(0, 0), (5, 0), (10, 0), (0, 5), (0, 10), (5, 10) mol%. T_g decreased when CaO was replaced with SrO. The results suggested that Sr had a higher affinity for the boron sub-network. These glasses showed rapid HAp formation. Stabilization of the borate network helped in controlling the boron release and enhances bone formation [65]. It can be concluded that the composition of glasses with alkaline earth oxides such as CaO, SrO enhances crystallization, insulating and optical properties, chemical durability and mechanical and thermal stability of the glass [5, 15].

The summary of the literature survey is given in Table 2.1. Table 2.2 reports the T_g, T_c, T_p, E_g, E_u values of different silicate, borate, and borosilicate glasses.

Table 2.1: Summary of literature review.

Author & Reference	Glass composition	Remarks	Applications
Hench et al. (1991) [22]	$SiO_2-Na_2O-CaO-P_2O_5$ (known as 45S5)	High bioactivity but slow degradation rate and failure in mechanical strength	Form bone matrix and used in middle ear prosthesis
Ohura et al. (1991) [42]	$CaO-SiO_2$, $CaO-SiO_2-CaF_2$ and $CaO-SiO_2-P_2O_5$	Bone bonding ability and strength is same of both P-free and P-containing glass	-
Fredholm et al. (2010) [43]	$SiO_2-P_2O_5-CaO-SrO-Na_2O$	Small change in chemical structure and expansion occurred, T_g value decreased and weak glass structure	-
Huang et al. (2011) [44]	$SiO_2-Na_2O-K_2O-MgO-CaO-P_2O_5$ (known as 13-93)	Requisite mechanical, compressive strength, bioactive, proliferation supported but rate of conversion to hydroxyapatite layer (HAp) reduced	Applicable in repair and regeneration of load bearing bones
Jha et al. (2016) [45]	$SiO_2-K_2O-CaO-MgO$	Enhanced chemical durability but retarded bioactive properties	-
Hesaraki et al. (2010) [46]	$SiO_2-P_2O_5-CaO-SrO$	More degradable glass produced, T_g depends on Sr concentration but bioactive properties retarded	-
Richard et al. (2000) [51]	All SiO_2 replaced with B_2O_3 in 45S5 (known as 45S5B1)	Faster conversion to HAp, enhanced network connectivity, higher degradation rate but decreased strength	-
Abdel et al. (2007) [53]	$Na_2O-B_2O_3-BaO-MgO$	E_g and E_u increased as MgO/BaO increased, better optical properties	Used in wave-guide applications
Liang et al. (2008) [54]	$Na_2O-CaO-B_2O_3$	Partially/fully converted to HAp, partially converted has higher metabolic activity than completely converted borate glass	Used in bone tissue engineering and favourable for characteristics for cell viability
Abdelghany et al. (2013) [25]	$B_2O_3-CaO-Na_2O-Li_2O-K_2O$	B_2O_3 is hygroscopic oxide, highly soluble in water and corrosive but corrosive nature improved with the addition of alkali oxide	Applicable in biomedical field

Author & Reference	Glass composition	Remarks	Applications
Abdelghany et al. (2016) [55]	$B_2O_3-CaO-Na_2O-SrO$	Enhanced bioactivity and apatite formation depends on SrO concentration	-
Brink et al. (1997) [56]	$Na_2O-K_2O-MgO-CaO-B_2O_3-P_2O_5-SiO_2$	Bioactive, very reactive, maintained mechanical strength but lower chemical durability	Suitable for biomedical applications
Huang et al. (2006) [52]	$Na_2O-CaO-SiO_2-B_2O_3-P_2O_5$	Faster conversion to HAp	-
Brown et al. (2009) [57]	$Na_2O-CaO-B_2O_3-SiO_2-P_2O_5$	Enhanced conversion rate, inhibition of cell proliferation in cultures	-
Fu et al. (2010) [39]	$SiO_2-B_2O_3-Na_2O-K_2O-MgO-CaO-P_2O_5$	Faster conversion to HAp, enhanced bioactivity, degradation rate and network connectivity but strength decreased	Suitable for repairing defects present in bones
Prasad et al. (2019) [58]	$SiO_2-B_2O_3-Na_2O-CaO-P_2O_5$	Thermal stability better than its borate counterparts, improved in-vitro cell proliferation, antibacterial properties and biomineralization ability	-
Mondal et al. (2013) [59]	$ZrO_2-CaO-P_2O_5-Na_2O-SiO_2$	Mechanical strength and fracture toughness increased, better mechanical strength and compatibility up to 10 wt% ZrO_2	Suitable in load bearing applications
Samudrala et al. (2016) [60]	$B_2O_3-SiO_2-Na_2O-CaO-ZrO_2$	Zr gives strength to the glass, higher chemical reactivity and good bioactivity	Promising bioactive material and applicable in medical field
Agathopoulos et al. (2006) [61]	$SiO_2-B_2O_3-CaO-MgO-P_2O_5-Na_2O-CaF_2$	Bioactive in nature	-
Belluci et al. (2017) [62]	$Na_2O-K_2O-CaO-P_2O_5-SiO_2$	Improved bioactivity and good mechanical properties	Bone formation promoted, bone resorption reduced and are used in dental implants and bone regeneration
Kargozar et al. (2019) [50]	$SiO_2-P_2O_5-CaO-Na_2O-SrO$	Enhanced rate of HAp formation, Sr^{2+} ions have antibacterial properties and reduced bone resorption	Suitable in dental applications

Author & Reference	Glass composition	Remarks	Applications
Gautam et al. (2020) [63]	SrO-TiO_2-SiO_2-B_2O_3-TeO_2	NBOs are formed due to decrease in fraction of BO_4 units and E_g values decreased because of increased NBOs	-
Mohini et al. (2018) [48]	$B_2O_3 - SiO_2 - CaO - Na_2O - SrO$	NBOs are created and decreased value of E_g	-
Kaur et al. (2019) [15]	$CaO - MgO - SrO - B_2O_3 - Al_2O_3 - SiO_2$	With the addition of modifiers, structural changes occurred and also NBOs reduced	Used for optical applications
Khan et al. (2017) [9]	$SiO_2 - B_2O_3 - Y_2O_3 - CaO - ZrO_2$	NBOs and tendency of phase separation increased and structural changes occurred	Applicable in optical switches
Walia et al. (2021) [5]	$SrO - BaO - SiO_2 - B_2O_3 - ZrO_2$	Tendency of phase separation decreased and good insulating properties	Used in SOFCs as sealants
Fujikura et al. (2012) [64]	$SiO_2 - P_2O_5 - CaO - SrO - Na_2O$	Faster dissolution rate, significant effects bioactivity and structure of the glass	-
Tainio et al. (2020) [65]	$SiO_2 - B_2O_3 - CaO - Na_2O - P_2O_5 - MgO - SrO$	Rapid HAp formation, enhanced bone formation, helps in bone release and stabilizing borate network and better thermal properties	Applicable in bone tissue engineering

Table 2.2: The values of T_g, T_c, T_p, E_g and E_u of different glasses.

Glass composition	T_g ($^\circ C/min$)	T_c ($^\circ C/min$)	T_p ($^\circ C/min$)	E_g (eV)	E_u (eV)	Reference
Na_2O-K_2O-CaO-P_2O_5-SiO_2-MgO-SrO	655-720	832-860	865-883	-	-	[62]
SiO_2-B_2O_3-CaO-Na_2O-P_2O_5-MgO-SrO	472-529	647-691	725-795	-	-	[65]
SrO-BaO-SiO_2-B_2O_3-ZrO_2	543-705	-	-	3.27-3.83	0.24-033	[5]
CaO-MgO-SrO-B_2O_3-Al_2O_3-SiO_2	-	-	-	5.83-6.01	0.62-0.86	[15]
SiO_2-K_2O-CaO-MgO	-	-	-	3.46-3.72	0.11-0.16	[45]
B_2O_3-SiO_2-CaO-Na_2O-SrO	-	-	-	2.36-2.98	-	[48]
SiO_2-P_2O_5-CaO-SrO-Na_2O	496-539	640-665	-	-	-	[64]
SiO_2-P_2O_5-Na_2O-K_2O-MgO-CaO	524-588	-	-	-	-	[40]
SiO_2-B_2O_3-Y_2O_3-CaO-ZrO_2	-	-	-	3.74-3.84	0.14-0.17	[9]
SiO_2-CaO-MgO-Na_2O-K_2O-Al_2O_3	-	-	-	3.26-3.57	0.30-0.32	[18]
Na_2O-SrO-B_2O_3-SiO_2	578-582	-	-	-	-	[66]
SrO-TiO_2-SiO_2-B_2O_3-TeO_2	-	-	-	3.31-3.48	0.28-0.30	[63]

Chapter 3

Gaps in literature and Objectives

3.1 Gaps in the literature

After the literature review, it can be concluded that a lot of work has been done on borosilicate glasses but still plenty of research is still in progress. Based on the literature review following gaps have been found:

1. Many borosilicate glasses have been studied for the effect of SrO on borosilicate glasses and ZrO_2 on borosilicate glasses but the combined effect of SrO and ZrO_2 on borosilicate glasses have been limited.

2. The study of thermal, structural and optical properties has been limited either to SrO borosilicate glasses or ZrO_2 borosilicate glasses. However, studies on SrO and ZrO_2 borosilicate glasses are rare.

3.2 Objectives

Based on the literature survey, the following objectives are proposed:
To study the thermal, optical and structural properties of $29SiO_2 - 20B_2O_3 - 24.5Na_2O - (24.5 - x)CaO - xSrO - 2ZrO_2$ glasses where, x=0, 5, 10, 15 wt% using differential thermal analysis (DTA), diffuse reflectance spectroscopy (DRS) and Fourier transform infrared spectroscopy (FTIR).

Chapter 4

Materials and Methods

4.1 Methodology

The samples were synthesized by melt-quench technique and the process of sample preparation is shown in Figure 4.1. Initially, stoichiometric amount of SiO_2, H_3BO_3, $CaCO_3$, Na_2CO_3, ZrO_2 and $SrCO_3$ were mixed properly for 2 hours. Then, mixture was heated till 500°C for 1 hour to allow decomposition of H_3BO_3 to B_2O_3. Further, the samples were melt at 1250°C where the temperature was held for 2 hours to get homogeneous mixing of the melt. By using copper plates, the melt was quenched in air. The sample composition and IDs are given in Table 4.1 and the synthesized samples are shown in Figure 4.2, where,1, 2, 3 and 4 represents SG1, SG2, SG3 and SG4 glass samples respectively. The synthesized samples are transparent and clear.

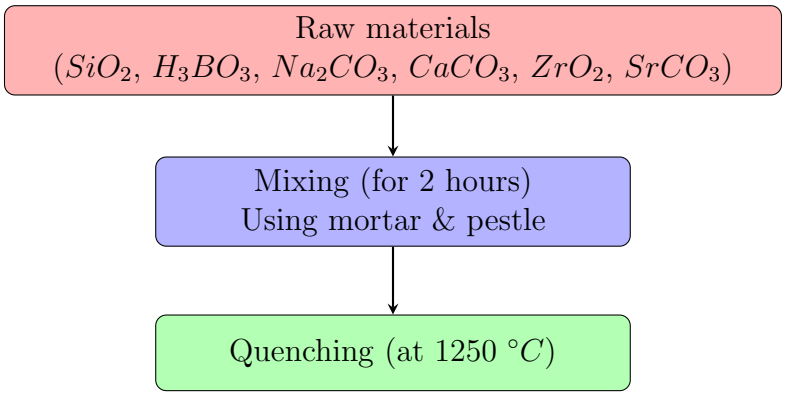

Figure 4.1: Flowchart of sample preparation

Table 4.1: IDs and composition in wt% of borosilicate glasses.

Sample ID	SiO_2	B_2O_3	Na_2O	CaO	SrO	ZrO_2
SG1	29.0	20.0	24.5	24.5	0.0	2.0
SG2	29.0	20.0	24.5	19.5	5.0	2.0
SG3	29.0	20.0	24.5	14.5	10.0	2.0
SG4	29.0	20.0	24.5	9.5	15.0	2.0

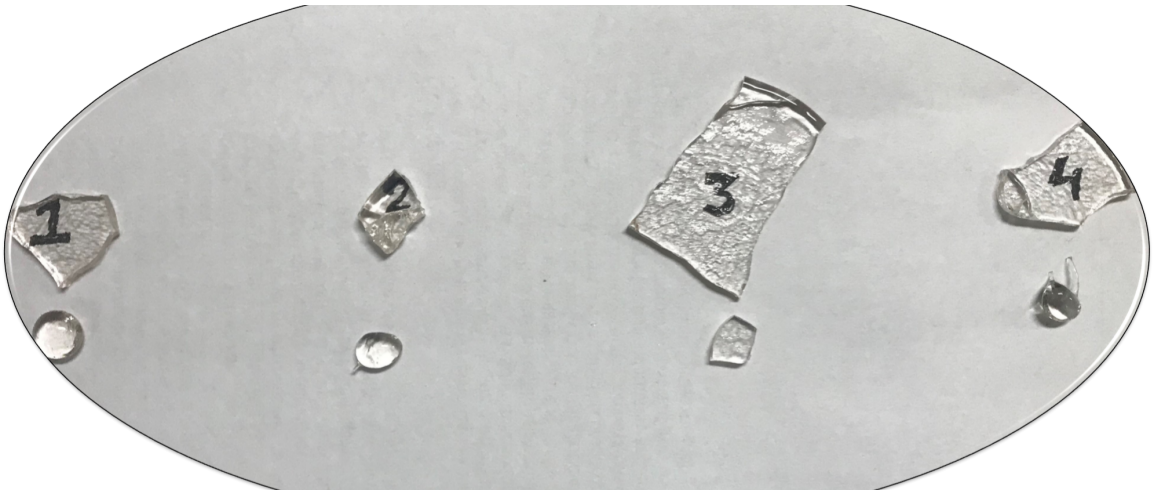

Figure 4.2: Synthesized borosilicate glass samples, where, 1, 2, 3 and 4 represents SG1, SG2, SG3 and SG4 glass samples.

The present study, reports the structural, thermal, and optical properties of SrO-ZrO_2 containing soda lime borosilicate glasses. Because of difference in the field strength of Sr and Ca, the substitution of Sr in place of Ca can influence the properties of the synthesized glasses.

4.2 Characterizations

4.2.1 Differential Thermal Analysis

Differential Thermal Analysis (DTA) technique is used to obtain characteristic temperatures of a glass sample [7]. DTA has a sample holder containing thermocouple, furnace, container, recording system. In differential manner, two thermocouples are joined together and further connected to differential amplifier. One thermocouple is positioned with the glass sample and other one into reference sample [7]. Alumina (Al_2O_3) is used as a reference material in the measurement [7, 12, 67]. In DTA, the sample under study along with an inert reference go through identical thermal cycles. Then, temperature difference between the reference and sample is observed [7, 11]. The differential temperature is represented with respect to temperature and then alteration in the sample whether exothermic or endothermic are observed in comparison to the reference material [7, 11]. The glass transition and crystallization temperatures for the synthesized glasses are determined from the DTA curve [7]. In the present study, DTA data is obtained by Perkin Elmer thermal analyzer (Model: Diamond TG/DTA) in nitrogen atmosphere at a continuous heating rate of 10°C/min from room temperature to 800°C.

4.2.2 Fourier Transform Infrared Spectroscopy

Fourier Transform Infrared Spectroscopy (FTIR) gives details about molecular level of the samples which helps in understanding the structure and dynamics of the sample [2, 68]. FTIR represents a method of IR spectroscopy where the sample is subjected to IR radiation. A part of the IR radiation is absorbed and a part is transmitted by the sample. When the frequency of incident IR radiations matches with the frequency of vibration of a chemical bond present in sample, it produces an IR band which is unique to that particular structural unit [7, 17]. In FTIR spectra, more than one bands of same bond at different wavenumbers can also be present. Since molecules can be vibrating in stretching mode, bending mode or rocking mode, etc. depending on their degree of freedoms. Shifting of bands in the spectra, give information about the bond strength of the functional groups and structural units present in the sample. Due to close vibrational frequencies, some bands in FTIR can be broad and are difficult to resolve [7]. FTIR spectra were recorded for all the prepared glass samples using Agilent Carry 660 instrument at room temperature with the wavenumber range from 4000 to 400 cm^{-1}. Fine powders with KBr powder were mixed for quantitative analysis. IR spectra were measured instantly after the preparation of disc to ignore moisture attack [17, 46, 69].

4.2.3 Diffusion Reflectance Spectroscopy

Diffusion Reflectance Spectroscopy (DRS) gives information about optical properties of glass samples [13]. This is used for the determination of the band gap of the samples which can either be direct or indirect [13]. When UV-visible light is incident on the samples, it passes through it and gives information about optical band gap of sample [7]. In transitions, interactions of incident radiations with the valence band of the sample occurs which excites the electrons from valence to the conduction band by gaining band gap [13, 68]. UV–visible spectra of all prepared samples in the form of powder was recorded in diffused reflectance mode on HITACHI U-3900 H by using double beam spectrophotometer with the wavelength range from 200-800 nm. The samples were scanned with the speed of 120 nm/min and with the 0.2 nm resolution of the instrument. The instrument was calibrated before taking the measurements with the use of standard sample (barium sulphate) [12].

Chapter 5

Results and Discussion

5.1 Differential Thermal Analysis

DTA curves give information regarding the glass transition temperature (T_g), onset crystallization temperature (T_c) and peak crystallization temperature (T_p) [7, 11].

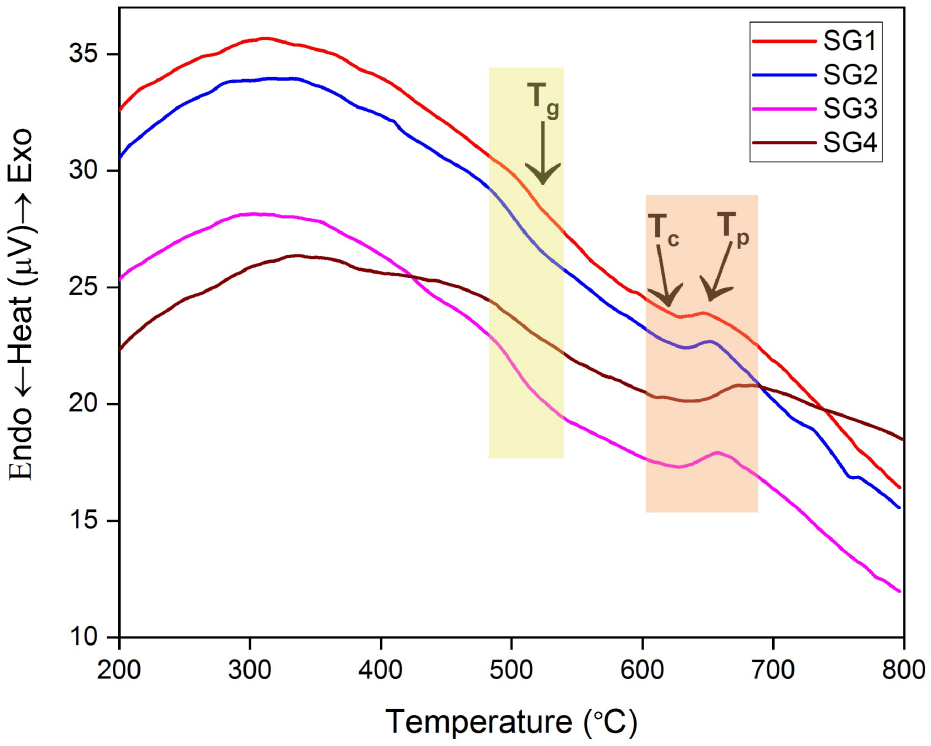

Figure 5.1: The DTA curves of the synthesized samples obtained at a heating rate of 10 $°C/min$.

At a constant heating rate, the characteristic temperatures give useful information about structure of the samples although it is a heating rate dependent technique [12]. The DTA curves of the synthesized samples attained at a heating rate of 10 °C/min are given in Figure 5.1. The onset of first endothermic peak in the DTA curve corresponds to T_g. Crystallization is observed as an exothermic peak, where T_c is the onset of the exothermic peak and the peak corresponds to T_p [26].The curve of glass samples

is characterized by (a) a change in baseline between 465°C and 500°C which represents T_g and (b) an exothermic peak between 625°C and 660°C representing crystallization. The values of T_g, T_c and T_p of synthesized glass samples are written in Table 5.1. T_g increases from SG1 to SG3, i.e, with the increase in the amount of Sr from 0 wt% to 10 wt%. The increase in viscosity of melt with the increase in the amount of Sr in glass melt causes an increase in T_g [70]. The increase in T_g indicates reduction in NBOs in the structure of glass samples [11]. On the other hand, when the amount of Sr increases from 10 wt% to 15 wt%, i.e. SG3 to SG4, then there is a decrease in T_g. The decrease in T_g indicates the creation of NBOs which means that modifiers break the glass network and make the glass structure weak [11, 12]. Variation in T_g with the increasing amount of SrO is shown in the Figure 5.2.

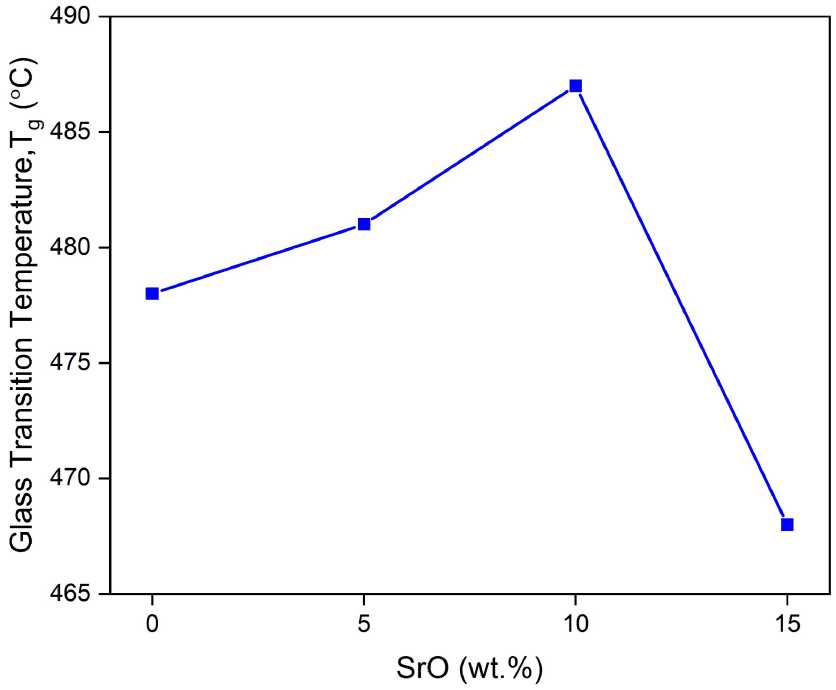

Figure 5.2: Variation of glass transition temperature (T_g) with the concentration of SrO.

Crystallization is a combination of nucleation and crystal growth [3]. In synthesized glasses, T_p increases with the increase in Sr concentration whereas T_c does not follow any regular trend.

Table 5.1: The values of T_g, T_c and T_p of the synthesized glass samples.

Sample ID	T_g $(°C/min)$	T_c $(°C/min)$	T_p $(°C/min)$
SG1	478	626	645
SG2	481	632	650
SG3	487	629	657
SG4	468	646	673

5.2 Fourier Transform Infrared Spectroscopy

Fourier Transform Infrared Spectroscopy (FTIR) provides details about the structural units present in a sample. It is used to determine the wavelength at which the material absorbs or transmits

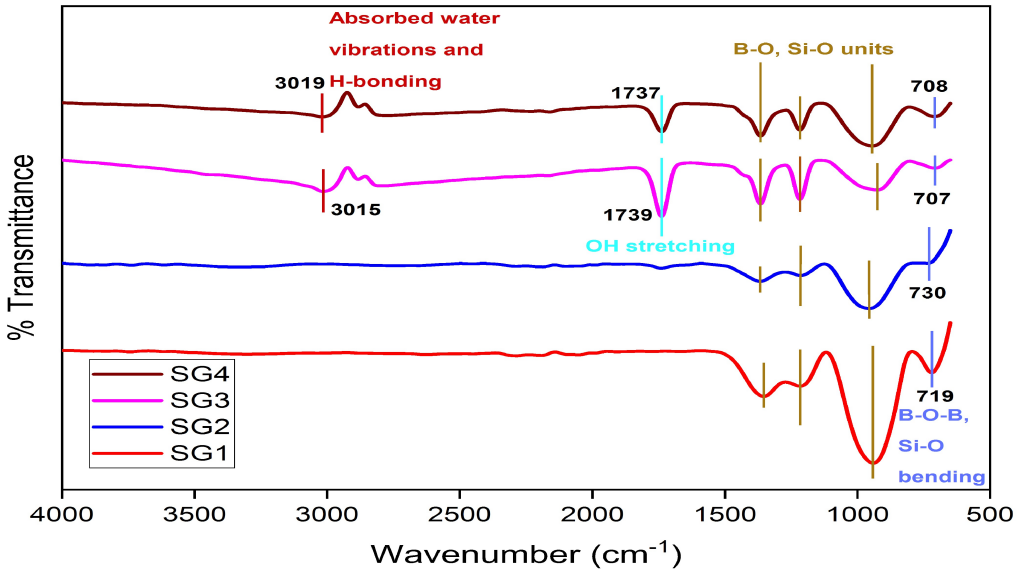

Figure 5.3: FTIR spectra of all glass samples.

infrared (IR) radiation [68], i.e. it is used to study the interaction between IR radiation and the sample [7]. The FTIR spectra of glass samples SG1, SG2, SG3 and SG4 are shown in Figure 5.3. The FTIR spectra consists of six major bands in the range 4000-600 cm^{-1}. There are some changes in the intensity of bands because of changes in the Sr/Ca ratio in the glass composition. The two bands at 1739-1737 and 3019-3015 cm^{-1} are due to the absorption of moisture from surroundings [71]. The band 1739-1737 cm^{-1} corresponds to molecular water and hydoxyl (OH) group stretching mode [21, 72]. The band 3019-3015 cm^{-1} corresponds to the absorbed water vibrations and hydrogen bonding [2, 13, 24, 71, 72]. With the increasing Sr content in the glass samples the tendency to absorb moisture from the surrounding increases. The band located at 730-700 cm^{-1} corresponds to

the Si-O bending [65, 71] and B-O-B bending vibrations in borate network [60, 71, 73]. The band centre and intensities are dependent on the SrO concnetration. The bands in between 1400-900 cm^{-1} is assigned to the vibrations of B-O and Si-O units [43, 55, 61, 65, 72]. B-O and Si-O bands are very close. There might be some overlapping of merged bands due to different units [74]. In order to differentiate different the structural units, deconvolution is performed for the region 1400-900 cm^{-1}. The centre intensities and areas are given in Table 5.2.

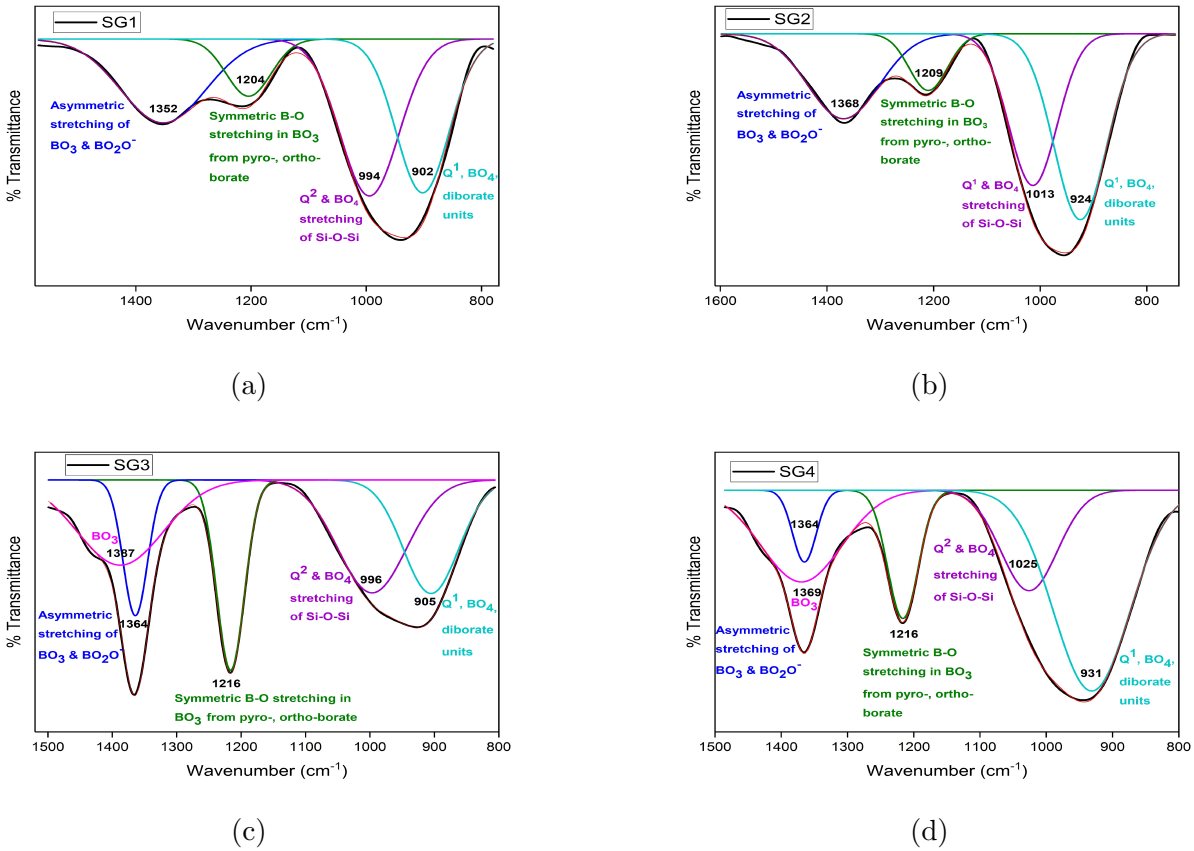

Figure 5.4: Deconvoluted FTIR spectra of (a) SG1, (b) SG2, (c) SG3, and (d) SG4.

Table 5.2: The centre intensities and area of the deconvoluted peaks.

Sample Id	Centre intensities (cm^{-1}) of the deconvoluted peaks and corresponding area, A (in brackets)				
SG1	902 (30)	994 (34.17)	1204 (9.5)	1352 (26.32)	-
SG2	924 (38.68)	1013 (28.85)	1209 (8.55)	1368 (23.92)	-
SG3	905 (21.14)	996 (26.32)	1216 (17.64)	1364 (11.22)	1387 (23.68)
SG4	931 (45.15)	1025 (16.83)	1216 (11.63)	1364 (5.04)	1369 (21.35)

The deconvoluted peaks shown in Figure 5.4 possess bands in the range 931-902, 1025-994, 1216-1203, 1368-1352 and 1387-1369 cm^{-1}. The deconvoluted bands in the range 1025-902 cm^{-1} cor-

responds to different silicate Q^n structural units [5]. The bands 931-902 cm^{-1} are assigned to Q^1 structural unit, while the 1025-994 cm^{-1} bands belong to the Q^2 structural unit [5]. The bands in the 1025-902 cm^{-1} region also represent vibrations because of the BO_4 structural units. The 931-902 cm^{-1} can be assigned to the B-O bonds stretching in BO_4 units of diborate groups. The stretching of B-O bonds in BO_4 units from tri-borate, tetra-borate, penta-borate groups are present at 1025-994 cm^{-1} [75, 76]. The 1216-1204 cm^{-1} band represents stretching of B-O bonds in BO_3 from pyro-borate, ortho-borate groups [75, 76, 77]. The band at 1387-1352 cm^{-1} represents asymmetric stretching of BO_3 and BO_2O^- [5, 75, 76]. Summary of the borate bands is given in Table 5.3.

In order to study the impact of the SrO/CaO ratio on boron units, it is important to calculate

Table 5.3: The assignment of bands in region 900-1400 cm^{-1} obtained from deconvoluted FTIR spectra of all glass samples.

Wavenumber (cm^{-1})				Assignments	Reference
SG1	SG2	SG3	SG4		
902	924	905	931	Q^1, B-O bonds in BO_4 from tri-borate, tetra-borate, penta-borate groups	[5, 75, 76]
994	1013	996	1025	Q^1, B-O bonds in BO_4 from diborate groups	[5, 76]
1204	1209	1216	1216	B-O in BO_3 from pyro-borate and ortho-borate groups	[75, 76, 77]
1352	1368	1364	1364	Asymmetric stretching of BO_3 and BO_2O^-	[5, 75, 76]
-	-	1387	1369	Asymmetric stretching of BO_3	[5]

the fraction of tetrahedral coordinated boron atoms (N_4). In order to calculate N_4, relative areas of BO_3 and BO_4 units are needed. The relative areas of BO_3 are calculated by the following equation (equation 5.1):

$$A(BO_3) = A(1216to1204) + A(1387to1352) \tag{5.1}$$

Since, there is an overlap between the vibrations of Si-O and BO_4, relative areas corresponding to Si-O needs to be considered while calculating relative areas of BO_4 units (equation 5.2):

$$A(BO_4) = \alpha[A(931to932) + A(1025to994)] \tag{5.2}$$

Where, α is the ratio of $B_2O_3/(2B_2O_3 + SiO_2)$. The fraction of BO_4 units can be calculated by (equation 5.3):

$$N_4 = \frac{A(BO_4)}{A(BO_4) + A(BO_3)} \tag{5.3}$$

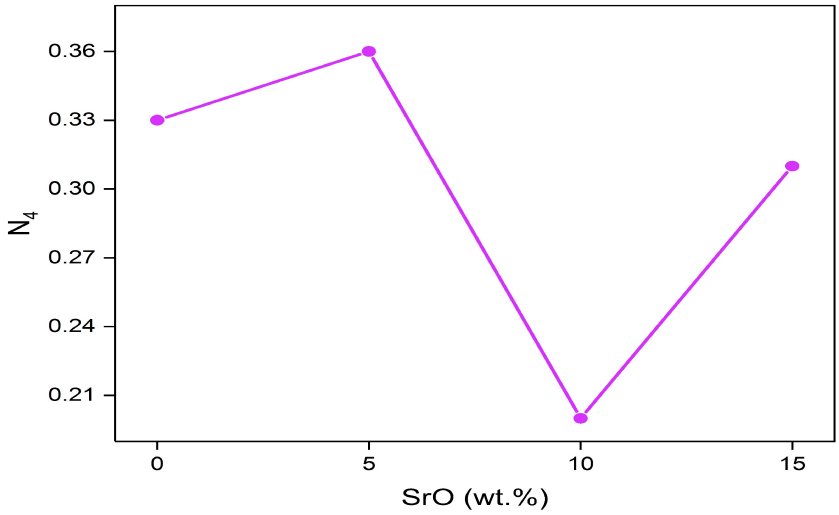

Figure 5.5: The variation of N_4 values with respect to the variation in the concentation of SrO in the glass composition

The calculated values of N_4 are shown in Figure 5.5.

It becomes clear that N_4 increases from SG1 to SG2, but then it decreases. This decrease can be associated with the conversion of BO_3 units into BO_4 and creation of NBOs in the glass network.

5.3 Diffuse Reflectance Spectroscopy

Diffusion Reflectance Spectroscopy (DRS) helps in the determination of optical properties like band gap, Urbach energy and refractive index of the samples. Both the direct and indirect optical band gaps are determined by using the following formula (equation 5.4)

$$F(R) = \frac{\alpha}{s} = \frac{(1-R)^2}{2R} \tag{5.4}$$

where, F(R) is Kubelka Munk function, R is reflectance, α is absorption coefficient and s is scattering coefficient [9, 12]. The optical band gap is determined by plotting $(F(R)h\nu)^N$ vs $h\nu$, where N=2 for direct, 1/2 for indirect as shown in Figure 5.6. The value of band gap (E_g) of the sample is calculated by the extrapolation of the curve on the x-axis corresponding to which $(F(R)h\nu)^N = 0$, [9, 12, 16]. The values of E_g for all the samples are written in Table 5.4. From the table 5.4, it is observed that both the direct and indirect optical band gaps are in the wide band gap semiconductor range. E_g increases with the increase in the amount of Sr. There is a very small increase in the direct band gap in comparison to the indirect band gap. But the existence of mixed modifier effect in the borosilicate

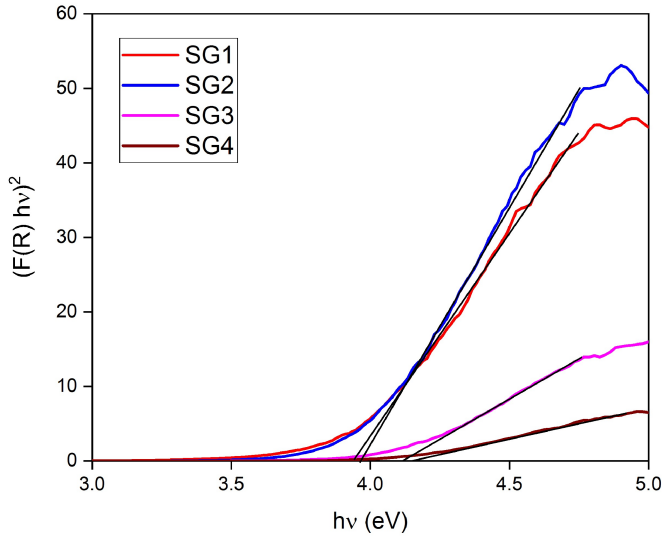

(a)

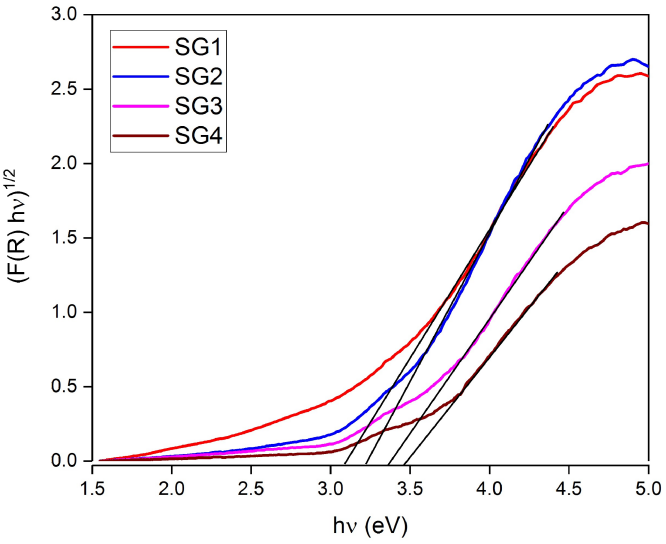

(b)

Figure 5.6: Optical (a) direct and (b) indirect bandgap of the samples.

glasses can result in an increase in the optical band gap with the addition of a heavier modifier [5]. Optical band gap depends upon the composition of glass samples [45]. The shift in energy bandgap to higher values can be due to formation of lesser number of the NBOs. The lower amount of NBOs causes decrease in 0 degree of localization of electrons and hence, reducing the donor centres in the glass matrix. Thus, due to the lower concentration of donor centres, an increase in E_g occurs [78]. The negative charge on NBO is of higher magnitude as compared to that on BO. When the ionicity of oxygen atoms is increased by changing them from bridging to non-bridging, then the top of valence

band is lifted resulting in decreased energy gap. On the contrary lesser NBOs should similarly cause an increase in the band gap [79, 80].

Table 5.4: Optical band gap, refractive index and Urbach energy of glass samples.

Sample Id	E_g (direct) (eV)	n_1	E_g (indirect) (eV)	n_2	E_u (eV)
SG1	3.94	2.18	3.07	2.38	0.39
SG2	3.96	2.18	3.22	2.34	0.28
SG3	4.11	2.15	3.36	2.31	0.32
SG4	4.17	2.14	3.47	2.28	0.28

Urbach energy provides information about the degree of structural disorder due to the randomness in amorphous materials. Localized states are formed by defects and disorder at or near conduction band level and the width of tail of localized states within E_g is given by Urbach energy [17, 45]. These defects can influence the formation of apatite layer on the glass surface. Different factors like dislocations, thermal vibrations and electric field of defects etc. can result in the tailing of energy states in the forbidden gap [79]. The Urbach energy (E_u) is calculated from the following formula (equation 5.5):

$$F(R) = \beta \exp\left(\frac{h\nu}{E_u}\right) \tag{5.5}$$

where, $h\nu$ is energy of photon and β is a constant called as band tailing parameter. Reciprocal of the slope of linear portion of the curve plotted between $\ln(F(R))$ vs $h\nu$ gives the value of Urbach energy (E_u) [9, 11, 12]. Urbach energy of a sample is always less than its band gap energy [18]. The defects in a sample increases as E_u increases of the sample [17]. The calculated values of Urbach energy for the samples are given in Table 5.4. It is observed that E_u is maximum for the sample having lowest E_g. Maximum E_U means maximum disorder in the glass and hence, maximum number of NBOs which leads to an open structure [15]. In the present case, defects are more in SG1 and SG3 but are less in SG2 and SG4.

The refractive index depends upon composition of the glass samples. Refractive index is considerably affected by the amount of NBOs since as the electron donating capacity is dependent on NBOs [15]. The refractive index is calculated from the formula written as below (equation 5.6):

$$\frac{n^2 - 1}{n^2 + 2} = 1 - \sqrt{\frac{E_g}{20}} \tag{5.6}$$

where, n is refractive index and E_g is band gap energy [81, 82]. The values of refractive index are written in Table 5.4. In Table 5.4, n_1 is refractive index calculated using direct band gap and n_2 is refractive index calculated using indirect band gap. The refractive index is maximum for SG1 and decreases as the amount of Sr increases. It is seen that n is inversely proportional to E_g. Refractive index is dependent on the density, co-ordination number, and NBOs present in the sample. Formation of NBOs results in more ionic bond, increasing the polarizability and thus increasing the band gap [79]. Thus, decrease in refractive index in the synthesized glasses implies that lesser NBOs are formed with the addition of SrO.

Chapter 6

Conclusion and Future Scope

6.1 Conclusion

The focus of the present work was to study thermal, optical and structural properties of $29SiO_2 - 20B_2O_3 - 24.5Na_2O - (24.5 - x)CaO - xSrO$, x=0, 5, 10, 15 wt% glasses prepared by melt-quench technique. These properties are investigated by using various techniques. Following conclusions are drawn from the results:

1. DTA results shows increase in T_g values when amount of SrO increases from 0 to 10 wt%, i.e. from SG1 to SG3 which could be due to the reduction in NBOs in the glass structure. But when the amount of SrO increases from 10 to 15 wt%, i.e. from SG3 to SG4 then there is decrease in T_g values which can be a result of increase in NBOs in the glass structure.

2. FTIR spectra consists of bands corresponding to Si-O and B-O bonds, SiO_4, BO_4 and BO_3 units. Further deconvolution of the peaks is performed to differentiate different units as there is some overlapping of Si-O and B-O bands. The calculated N_4 values show increase from SG1 to SG2 and then decline due to BO_3 units conversion into BO_4 and creation of NBOs.

3. E_g increases as the amount of SrO increases due to mixed modifier effect or creation of lesser NBOs. Refractive index decreases with the addition SrO which implies that lesser NBOs are formed.

Thus, it can be concluded that addition of SrO in place of CaO increases the connectivity in the glass network to a certain extent.

6.2 Future Scope

The composition of theses glasses is very similar to the bioglass discussed in the literature. To study the bioactive properties of the glasses in-vitro studies are to be carried out by dipping them in simulated body fluid (SBF). After soaking, samples will be analyzed using XRD, FTIR, SEM with energy dispersive x-ray spectroscopy (EDS), pH and weight change.

Bibliography

[1] G. Kaur, O. P. Pandey, K. Singh, D. Homa, B. Scott, G. Pickrell, A review of bioactive glasses: their structure, properties, fabrication and apatite formation, Journal of Biomedical Materials Research Part A 102 (1) (2014) 254–274.

[2] C. Gautam, S. Dixit, A. Madheshiya, Synthesis and structural properties of lead strontium titanate borosilicate glasses with addition of chromium trioxide and graphene nanoplatlets, Spectroscopy Letters 48 (4) (2015) 280–285.

[3] J. E. Shelby, Introduction to glass science and technology, Royal Society of Chemistry, 2020.

[4] H. R. Fernandes, A. Gaddam, A. Rebelo, D. Brazete, G. E. Stan, J. M. Ferreira, Bioactive glasses and glass-ceramics for healthcare applications in bone regeneration and tissue engineering, Materials 11 (12) (2018) 2530.

[5] T. Walia, K. Singh, Mixed alkaline earth modifiers effect on thermal, optical and structural properties of $SrO - BaO - SiO_2 - B_2O_3 - ZrO_2$ glass sealants, Journal of Non-Crystalline Solids 564 (2021) 120812.

[6] F. Steudel, S. Loos, B. Ahrens, S. Schweizer, Quantum efficiency and energy transfer processes in rare-earth doped borate glass for solid-state lighting, Journal of Luminescence 170 (2016) 770–777.

[7] P. Jha, K. G. Singh, Preparation and characterization of $SiO_2 - CaO - MgO - K_2O$ glasses as biomaterials, Ph.D. thesis (2017).

[8] S. W. Verbruggen, S. Ribbens, T. Tytgat, B. Hauchecorne, M. Smits, V. Meynen, P. Cool, J. A. Martens, S. Lenaerts, The benefit of glass bead supports for efficient gas phase photocatalysis: case study of a commercial and a synthesised photocatalyst, Chemical engineering journal 174 (1) (2011) 318–325.

[9] S. Khan, G. Kaur, K. Singh, Effect of ZrO_2 on dielectric, optical and structural properties of yttrium calcium borosilicate glasses, Ceramics International 43 (1) (2017) 722–727.

[10] G. Kaur, S. G. Waldrop, V. Kumar, O. P. Pandey, N. Sriranganathan, An introduction and history of the bioactive glasses, in: Biocompatible Glasses, Springer, 2016, pp. 19–47.

[11] M. Shakeri, M. Rezvani, Optical band gap and spectroscopic study of lithium alumino silicate glass containing Y^{3+} ions, Spectrochimica Acta Part A: Molecular and Biomolecular Spectroscopy 79 (5) (2011) 1920–1925.

[12] S. Singh, G. Kalia, K. Singh, Effect of intermediate oxide (Y_2O_3) on thermal, structural and optical properties of lithium borosilicate glasses, Journal of Molecular Structure 1086 (2015) 239–245.

[13] C. Gautam, A. K. Yadav, Synthesis and optical investigations on (Ba, Sr) TiO_3 borosilicate glasses doped with La_2O_3 (2013).

[14] G. V. Rao, H. Shashikala, Optical and mechanical properties of calcium phosphate glasses, Glass Physics and Chemistry 40 (3) (2014) 303–309.

[15] M. Kaur, G. Kaur, O. P. Pandey, V. Kumar, Effect of CaO/MgO ratio on the optical and theoretical parameters of alumino-borosilicate glasses, International Journal of Applied Glass Science 10 (2) (2019) 259–271.

[16] A. Kaur, S. Khan, D. Kumar, V. Bhatia, S. Rao, N. Kaur, K. Singh, A. Kumar, S. P. Singh, Effect of MnO on structural, optical and thermoluminescence properties of lithium borosilicate glasses, Journal of Luminescence 219 (2020) 116872.

[17] C. Gautam, S. Das, S. Gautam, A. Madheshiya, A. K. Singh, Processing and optical characterization of lead calcium titanate borosilicate glass doped with germanium, Journal of Physics and Chemistry of Solids 115 (2018) 180–186.

[18] G. Sharma, K. Singh, Dielectric and optical properties of glasses and glass-ceramics synthesized from agro-food wastes, Materials Chemistry and Physics 246 (2020) 122754.

[19] A. Silva, C. Queiroz, S. Agathopoulos, R. Correia, M. Fernandes, J. Oliveira, Structure of $SiO_2 - MgO - Na_2O$ glasses by ftir, raman and 29Si MAS NMR, Journal of Molecular Structure 986 (1-3) (2011) 16–21.

[20] E. Fiume, J. Barberi, E. Verné, F. Baino, Bioactive glasses: from parent 45S5 composition to scaffold-assisted tissue-healing therapies, Journal of Functional Biomaterials 9 (1) (2018) 24.

[21] Z. Hajifathali, M. Amirhosseinian, The effect of substitution of CaO/MgO and CaO/SrO on in vitro bioactivity of sol-gel derived bioactive glass, International Journal of Biomedical and Biological Engineering 13 (6) (2019) 279–287.

[22] L. L. Hench, Bioceramics: from concept to clinic, Journal of the American Ceramic Society 74 (7) (1991) 1487–1510.

[23] L. L. Hench, The story of bioglass®, Journal of Materials Science: Materials in Medicine 17 (11) (2006) 967–978.

[24] A. HAMEED, Ftir and some physical properties of alkaline earth borate glasses containing heavy metal oxides, Int. J. Eng. Sci. Technol. 3 (2011) 6698–7005.

[25] A. Abdelghany, Novel method for early investigation of bioactivity in different borate bio-glasses, Spectrochimica Acta Part A: Molecular and Biomolecular Spectroscopy 100 (2013) 120–126.

[26] K. Schuhladen, X. Wang, L. Hupa, A. R. Boccaccini, Dissolution of borate and borosilicate bioactive glasses and the influence of ion (Zn, Cu) doping in different solutions, Journal of Non-Crystalline Solids 502 (2018) 22–34.

[27] M. Kaur, K. Singh, Review on titanium and titanium based alloys as biomaterials for orthopaedic applications, Materials Science and Engineering: C 102 (2019) 844–862.

[28] J. B. Park, J. D. Bronzino, Biomaterials: principles and applications (2002).

[29] J. Whitlow, A. Paul, A. Polini, Bioactive materials: Definitions and application in tissue engineering and regeneration therapy, in: Biocompatible Glasses, Springer, 2016, pp. 1–17.

[30] D. F. Williams, There is no such thing as a biocompatible material, Biomaterials 35 (38) (2014) 10009–10014.

[31] K. Shanmugam, R. Sahadevan, Bioceramics-an introductory overview, Fundamental Biomaterials: Ceramics (2018) 1–46.

[32] I. Thompson, L. Hench, Mechanical properties of bioactive glasses, glass-ceramics and composites, Proceedings of the Institution of Mechanical Engineers, Part H: Journal of Engineering in Medicine 212 (2) (1998) 127–136.

[33] R. K. Samudrala, P. A. Azeem, Preliminary biological evaluation of tantalum containing soda lime borosilicate bioactive glasses, Journal of Alloys and Compounds 810 (2019) 151853.

[34] S. Punj, K. Singh, Bioactive calcium silicate glass synthesized from sustainable biomass wastes, Biofuels, Bioproducts and Biorefining 14 (6) (2020) 1141–1151.

[35] C. Gao, S. Peng, P. Feng, C. Shuai, Bone biomaterials and interactions with stem cells, Bone research 5 (1) (2017) 1–33.

[36] J. Venkatesan, S.-K. Kim, Chitosan composites for bone tissue engineering—an overview, Marine drugs 8 (8) (2010) 2252–2266.

[37] L. L. Hench, R. J. Splinter, W. Allen, T. Greenlee, Bonding mechanisms at the interface of ceramic prosthetic materials, Journal of biomedical materials research 5 (6) (1971) 117–141.

[38] V. Aina, G. Malavasi, A. F. Pla, L. Munaron, C. Morterra, Zinc-containing bioactive glasses: surface reactivity and behaviour towards endothelial cells, Acta Biomaterialia 5 (4) (2009) 1211–1222.

[39] Q. Fu, M. N. Rahaman, H. Fu, X. Liu, Silicate, borosilicate, and borate bioactive glass scaffolds with controllable degradation rate for bone tissue engineering applications. I. preparation and in vitro degradation, Journal of biomedical materials research part A 95 (1) (2010) 164–171.

[40] E. Coon, A. M. Whittier, B. M. Abel, E. L. Stapleton, R. Miller, Q. Fu, Viscosity and crystallization of bioactive glasses from 45S5 to 13-93, International Journal of Applied Glass Science 12 (1) (2021) 65–77.

[41] O. Tsigkou, J. R. Jones, J. M. Polak, M. M. Stevens, Differentiation of fetal osteoblasts and formation of mineralized bone nodules by 45S5 bioglass® conditioned medium in the absence of osteogenic supplements, Biomaterials 30 (21) (2009) 3542–3550.

[42] K. Ohura, T. Nakamura, T. Yamamuro, T. Kokubo, Y. Ebisawa, Y. Kotoura, M. Oka, Bone-bonding ability of P_2O_5-free CaO· SiO_2 glasses, Journal of biomedical materials research 25 (3) (1991) 357–365.

[43] Y. C. Fredholm, N. Karpukhina, R. V. Law, R. G. Hill, Strontium containing bioactive glasses: glass structure and physical properties, Journal of Non-Crystalline Solids 356 (44-49) (2010) 2546–2551.

[44] T. Huang, M. Rahaman, N. Doiphode, M.-C. Leu, B. Bal, D. Day, X. Liu, Porous and strong bioactive glass (13-93) scaffolds fabricated by freeze extrusion technique, Materials Science and Engineering: C 31 (7) (2011) 1482–1489.

[45] P. Jha, K. Singh, Effect of MgO on bioactivity, hardness, structural and optical properties of $SiO_2 - K_2O - CaO - MgO$ glasses, Ceramics International 42 (1) (2016) 436–444.

[46] S. Hesaraki, M. Gholami, S. Vazehrad, S. Shahrabi, The effect of Sr concentration on bioactivity and biocompatibility of sol–gel derived glasses based on $CaO - SrO - SiO_2 - P_2O_5$ quaternary system, Materials Science and Engineering: C 30 (3) (2010) 383–390.

[47] A. Yao, D. Wang, W. Huang, Q. Fu, M. N. Rahaman, D. E. Day, In vitro bioactive characteristics of borate-based glasses with controllable degradation behavior, Journal of the American Ceramic Society 90 (1) (2007) 303–306.

[48] G. J. Mohini, N. Krishnamacharyulu, G. S. Baskaran, C. S. Rao, V. R. Kumar, N. Veeraiah, Influence of strontium on structure, bioactivity and corrosion behaviour of $B_2O_3 - SiO_2 - Na_2O - CaO$ glasses-investigation by spectroscopic methods, Optical Materials 84 (2018) 292–300.

[49] S. Motke, S. Yawale, S. Yawale, Infrared spectra of zinc doped lead borate glasses, Bulletin of Materials Science 25 (1) (2002) 75–78.

[50] S. Kargozar, M. Montazerian, E. Fiume, F. Baino, Multiple and promising applications of strontium (Sr)-containing bioactive glasses in bone tissue engineering, Frontiers in bioengineering and biotechnology 7 (2019) 161.

[51] M. N. Richard, Bioactive behavior of a borate glass (2000).

[52] W. Huang, D. E. Day, K. Kittiratanapiboon, M. N. Rahaman, Kinetics and mechanisms of the conversion of silicate (45S5), borate, and borosilicate glasses to hydroxyapatite in dilute phosphate solutions, Journal of Materials Science: Materials in Medicine 17 (7) (2006) 583–596.

[53] M. Abdel-Baki, F. Abdel-Wahab, A. Radi, F. El-Diasty, Factors affecting optical dispersion in borate glass systems, Journal of Physics and Chemistry of Solids 68 (8) (2007) 1457–1470.

[54] W. Liang, M. N. Rahaman, D. E. Day, N. W. Marion, G. C. Riley, J. J. Mao, Bioactive borate glass scaffold for bone tissue engineering, Journal of Non-Crystalline Solids 354 (15-16) (2008) 1690–1696.

[55] A. Abdelghany, M. Ouis, M. Azooz, H. ElBatal, G. El-Bassyouni, Role of SrO on the bioactivity behavior of some ternary borate glasses and their glass ceramic derivatives, Spectrochimica Acta Part A: Molecular and Biomolecular Spectroscopy 152 (2016) 126–133.

[56] M. Brink, The influence of alkali and alkaline earths on the working range for bioactive glasses, Journal of Biomedical Materials Research: An Official Journal of The Society for Biomaterials and The Japanese Society for Biomaterials 36 (1) (1997) 109–117.

[57] R. F. Brown, M. N. Rahaman, A. B. Dwilewicz, W. Huang, D. E. Day, Y. Li, B. S. Bal, Effect of borate glass composition on its conversion to hydroxyapatite and on the proliferation of MC3T3-E1 cells, Journal of Biomedical Materials Research Part A 88 (2) (2009) 392–400.

[58] S. Prasad, A. Gaddam, A. Jana, S. Kant, P. Sinha, S. Tripathy, K. Annapurna, J. M. Ferreira, A. R. Allu, K. Biswas, Structure and stability of high CaO-and P_2O_5-containing silicate and borosilicate bioactive glasses, The Journal of Physical Chemistry B 123 (35) (2019) 7558–7569.

[59] D. Mondal, S. So-Ra, B. T. Lee, Fabrication and characterization of $ZrO_2 - CaO - P_2O_5 - Na_2O - SiO_2$ bioactive glass ceramics, Journal of Materials Science 48 (5) (2013) 1863–1872.

[60] R. Samudrala, G. V. Reddy, B. Manavathi, P. A. Azeem, Synthesis, characterization and cytocompatibility of ZrO_2 doped borosilicate bioglasses, Journal of Non-Crystalline Solids 447 (2016) 150–155.

[61] S. Agathopoulos, D. Tulyaganov, J. Ventura, S. Kannan, M. Karakassides, J. Ferreira, Formation of hydroxyapatite onto glasses of the $CaO - MgO - SiO_2$ system with B_2O_3, Na_2O, CaF_2 and P_2O_5 additives, Biomaterials 27 (9) (2006) 1832–1840.

[62] D. Bellucci, A. Sola, R. Salvatori, A. Anesi, L. Chiarini, V. Cannillo, Role of magnesium oxide and strontium oxide as modifiers in silicate-based bioactive glasses: Effects on thermal behaviour, mechanical properties and in-vitro bioactivity, Materials Science and Engineering: C 72 (2017) 566–575.

[63] C. Gautam, A. Madheshiya, A. K. Singh, K. K. Dey, M. Ghosh, Synthesis, optical and solid NMR studies of strontium titanate borosilicate glasses doped with TeO_2, Results in Physics 16 (2020) 102914.

[64] K. Fujikura, N. Karpukhina, T. Kasuga, D. Brauer, R. Hill, R. Law, Influence of strontium substitution on structure and crystallisation of bioglass® 45S5, Journal of Materials Chemistry 22 (15) (2012) 7395–7402.

[65] J. Tainio, D. A. Salazar, A. Nommeots-Nomm, C. Roiland, B. Bureau, D. Neuville, D. Brauer, J. Massera, Structure and in vitro dissolution of Mg and Sr containing borosilicate bioactive glasses for bone tissue engineering, Journal of Non-Crystalline Solids 533 (2020) 119893.

[66] V. Eremyashev, D. Zherebtsov, L. Osipova, M. Brazhnikov, Effect of calcium, barium, and strontium on the thermal properties of borosilicate glasses, Glass and Ceramics 74 (9) (2018) 345–348.

[67] H. ElBatal, M. Azooz, E. Khalil, A. S. Monem, Y. Hamdy, Characterization of some bioglass-ceramics, Materials chemistry and physics 80 (3) (2003) 599–609.

[68] S. Das, A. Madheshiya, S. Gautam, C. Gautam, Fabrication and optical characterizations of lead calcium titanate borosilicate glasses, Journal of Non-Crystalline Solids 478 (2017) 16–22.

[69] H. Kamal, A. Hezma, Structure and physical properties of borosilicate as potential bioactive glasses, Silicon 10 (3) (2018) 851–858.

[70] A. K. Yadav, C. Gautam, P. Singh, Crystallization and dielectric properties of Fe_2O_3 doped barium strontium titanate borosilicate glass, RSC advances 5 (4) (2015) 2819–2826.

[71] S. Y. Marzouk, R. Seoudi, D. A. Said, M. S. Mabrouk, Linear and non-linear optics and FTIR characteristics of borosilicate glasses doped with gadolinium ions, Optical Materials 35 (12) (2013) 2077–2084.

[72] F. El-Batal, E. Khalil, Y. Hamdy, H. Zidan, M. Aziz, A. Abdelghany, FTIR spectral analysis of corrosion mechanisms in soda lime silica glasses doped with transition metal oxides, Silicon 2 (1) (2010) 41–47.

[73] S. Ferraris, A. Nommeots-Nomm, S. Spriano, E. Vernè, J. Massera, Surface reactivity and silanization ability of borosilicate and mg-sr-based bioactive glasses, Applied Surface Science 475 (2019) 43–55.

[74] H. Darwish, M. Gomaa, Effect of compositional changes on the structure and properties of alkali-alumino borosilicate glasses, Journal of materials science: materials in electronics 17 (1) (2006) 35–42.

[75] Y. Lai, Y. Zeng, X. Tang, H. Zhang, J. Han, H. Su, Structural investigation of calcium borosilicate glasses with varying Si/Ca ratios by infrared and raman spectroscopy, RSC advances 6 (96) (2016) 93722–93728.

[76] P. Pascuta, R. Lungu, I. Ardelean, FTIR and raman spectroscopic investigation of some strontium-borate glasses doped with iron ions, Journal of Materials Science: Materials in Electronics 21 (6) (2010) 548–553.

[77] M. Gaafar, S. Marzouk, Mechanical and structural studies on sodium borosilicate glasses doped with Er_2O_3 using ultrasonic velocity and ftir spectroscopy, Physica B: Condensed Matter 388 (1-2) (2007) 294–302.

[78] G. S. Baskaran, N. K. Mohan, V. V. Rao, D. K. Rao, N. Veeraiah, Influence of aluminium ions on physical properties of $PbO - P_2O_5 - As_2O_3$ glasses, The European Physical Journal Applied Physics 34 (2) (2006) 97–106.

[79] G. Kaur, O. Pandey, K. Singh, Effect of modifiers field strength on optical, structural and mechanical properties of lanthanum borosilicate glasses, Journal of Non-Crystalline Solids 358 (18-19) (2012) 2589–2596.

[80] M. Kaur, G. Kaur, O. Pandey, V. Kumar, Effect of CaO/MgO ratio on the optical and theoretical parameters of alumino-borosilicate glasses, International Journal of Applied Glass Science 10 (2) (2019) 259–271.

[81] R. El-Mallawany, M. D. Abdalla, I. A. Ahmed, New tellurite glass: Optical properties, Materials Chemistry and Physics 109 (2-3) (2008) 291–296.

[82] S. H. Alazoumi, S. A. Aziz, R. El-Mallawany, U. S. Aliyu, H. M. Kamari, M. H. M. M. Zaid, K. A. Matori, A. Ushah, Optical properties of zinc lead tellurite glasses, Results in Physics 9 (2018) 1371–1376.

Turnitin Originality Report

Processed on: 30-Jul-2021 04:52 +0530
ID: 1625586059
Word Count: 8197
Submitted: 1

Similarity Index
10%

Similarity by Source

Internet Sources:	4%
Publications:	7%
Student Papers:	4%

Simranjeet Thesis By Simranjeet Kaur

1% match (student papers from 09-Oct-2020)
Submitted to Thapar University, Patiala on 2020-10-09

1% match (student papers from 12-Sep-2020)
Submitted to Thapar University, Patiala on 2020-09-12

1% match (publications)
Gurbinder Kaur, Manoj Kumar, Anu Arora, O.P. Pandey, K. Singh. "Influence of Y2O3 on structural and optical properties of SiO2–BaO–ZnO–xB2O3–(10–x) Y2O3 glasses and glass ceramics", Journal of Non-Crystalline Solids, 2011

< 1% match (student papers from 07-Apr-2016)
Submitted to Thapar University, Patiala on 2016-04-07

< 1% match (Internet from 21-Jan-2021)
http://docplayer.net/36822930-Chapter-2-preparation-methods-and-characterization-techniques.html

< 1% match (Internet from 17-Oct-2020)
http://docplayer.net/44524963-Development-of-compactrio-based-pid-temperature-controller.html

< 1% match (Internet from 18-Dec-2019)
http://docplayer.net/50280526-1-introduction-2-experimental.html

< 1% match (publications)
Sakthi Prasad, Anuraag Gaddam, Anuradha Jana, Shashi Kant et al. " Structure and Stability of High CaO- and P O -Containing Silicate and Borosilicate Bioactive Glasses ", The Journal of Physical Chemistry B, 2019

< 1% match (Internet from 22-Jul-2019)
https://akademiai.com/doi/full/10.1007/s10973-011-1857-2

< 1% match (student papers from 20-Mar-2017)
Submitted to Institute of Graduate Studies, UiTM on 2017-03-20

< 1% match (Internet from 17-Feb-2019)
https://hal.archives-ouvertes.fr/hal-02004726/file/BiFeO3-nano-3b-rev1.pdf

< 1% match (publications)